Electronic Supplementary Material (ESI) for New Journal of Chemistry.
This journal is © The Royal Society of Chemistry and the Centre National de la Recherche Scientifique 2017

Electronic Supporting Information

Boratriazines: Inducing luminescence through boron incorporation into a terpy-type framework.

Muhammad Yousaf,[a] Nathan J. Yutronkie,[a] Raúl Castañeda,[a] Jacob A. Klein [a] and Jaclyn Brusso*,[a]

[a] Department of Chemistry and Biomolecular Sciences, University of Ottawa, Ottawa, Ontario K1N 6N5, Canada.

Contents (18 pages)

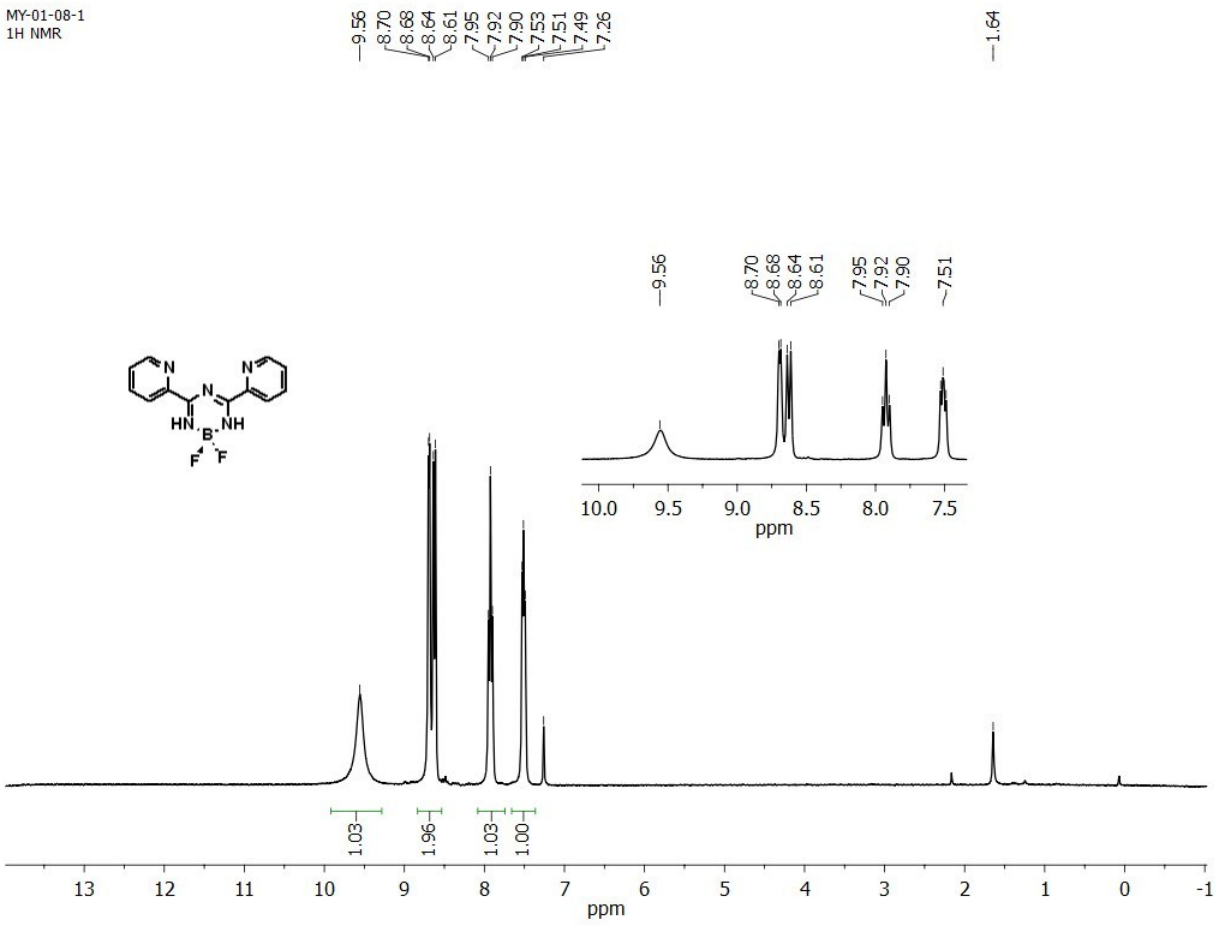

Figure S1. ^{1}H NMR spectrum of **F_2-Py_2BTA** in $CDCl_3$

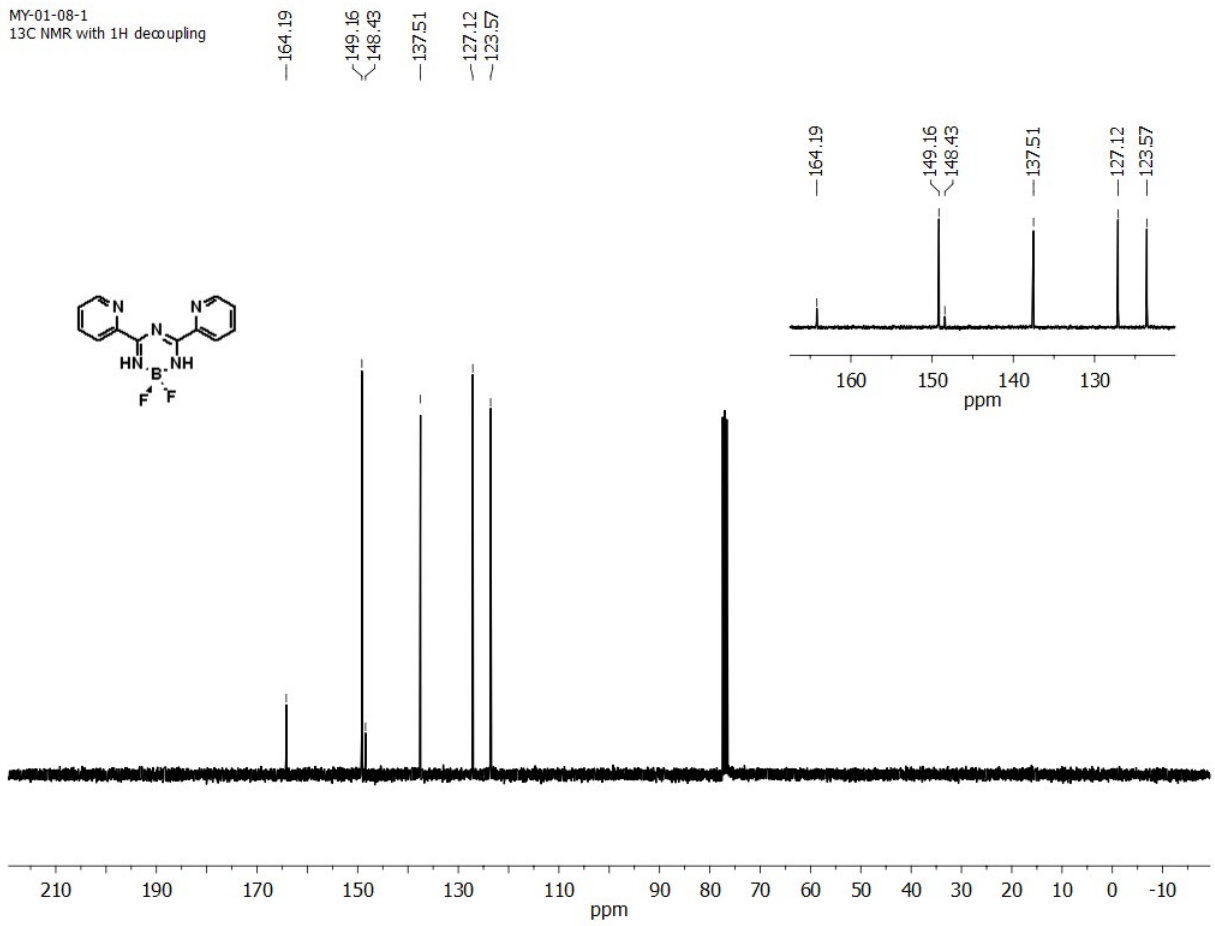

Figure S2. ^{13}C NMR spectrum of **F_2-Py_2BTA** in $CDCl_3$

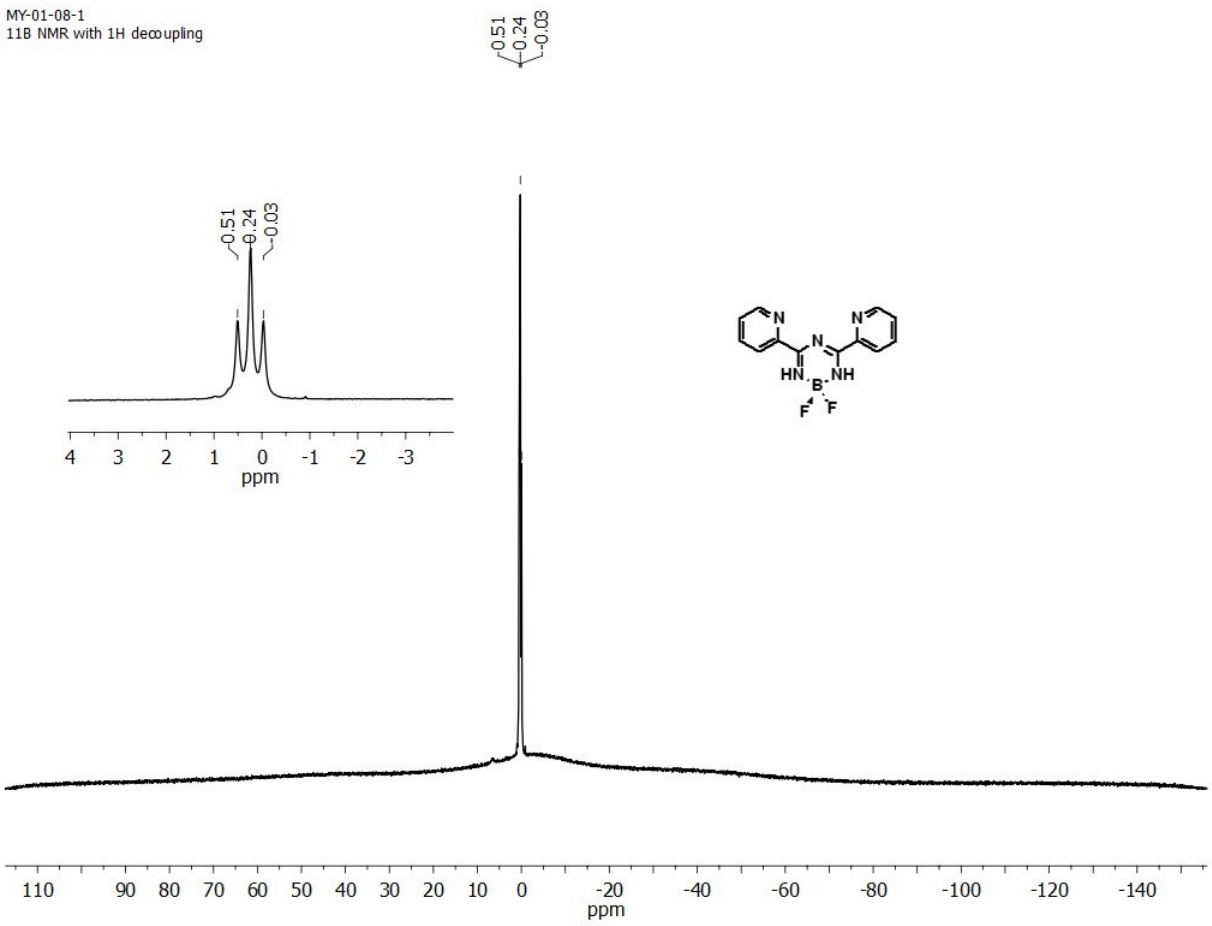

Figure S3. ^{11}B NMR spectrum of **F_2-Py_2BTA** in $CDCl_3$

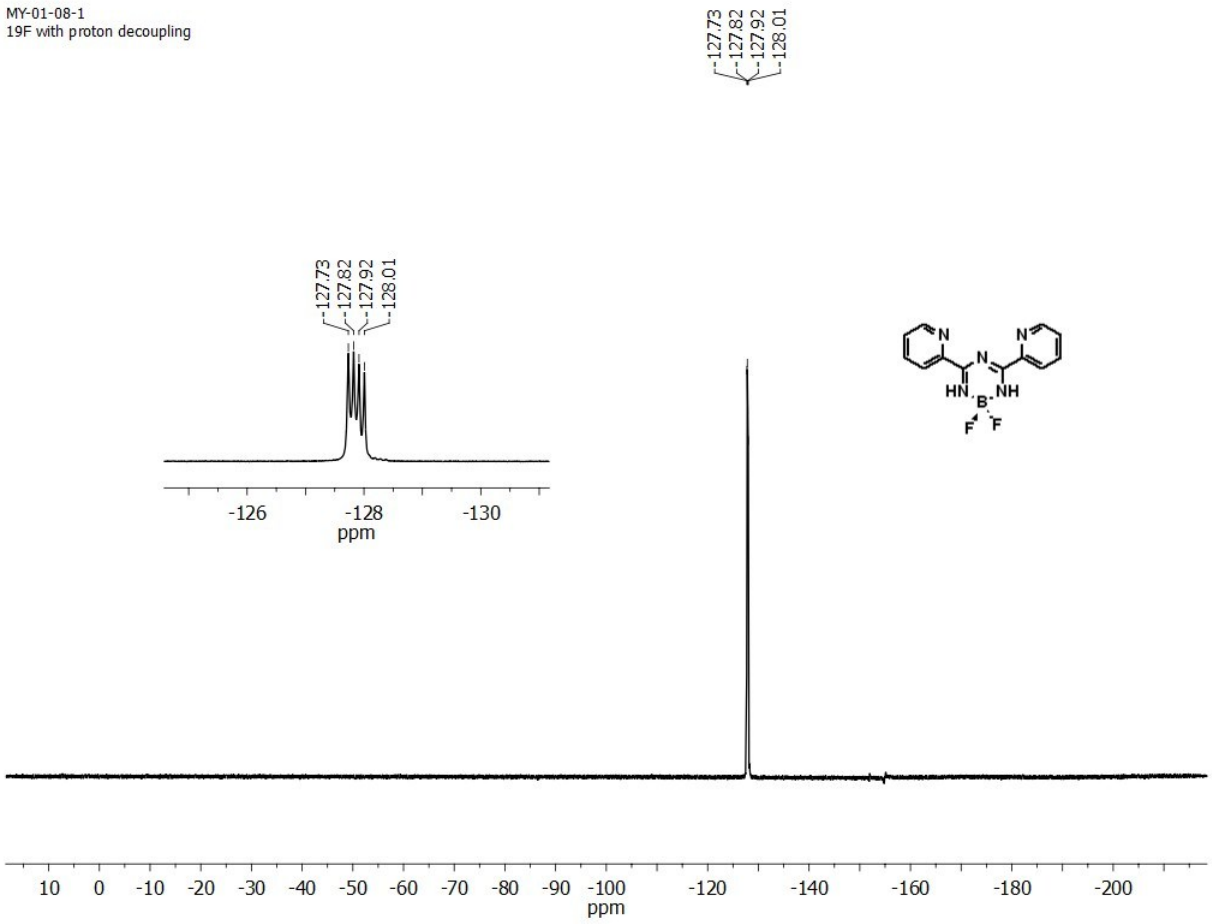

Figure S4. ^{19}F NMR spectrum of **F_2-Py_2BTA** in $CDCl_3$

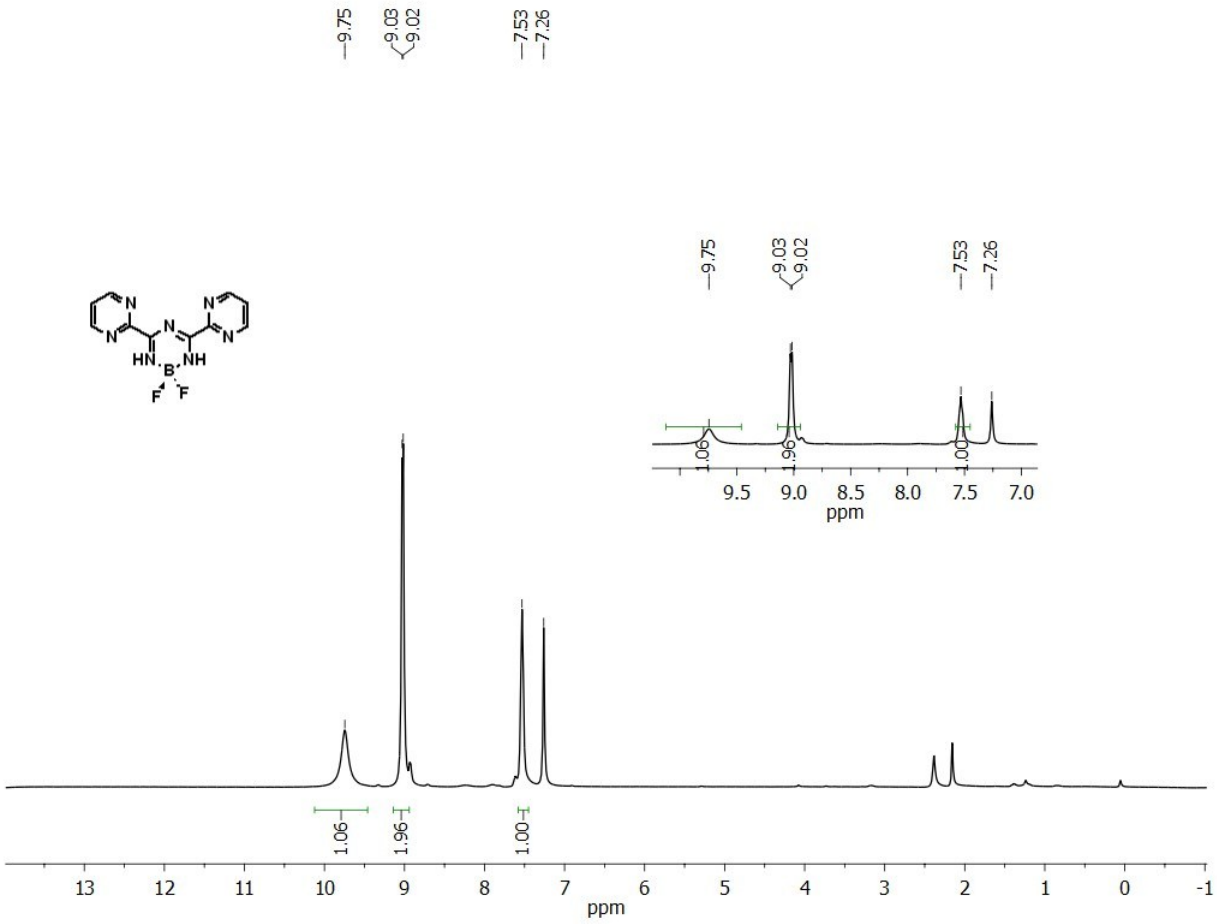

Figure S5. ^{1}H NMR spectrum of **F_2-Pm_2BTA** in $CDCl_3$

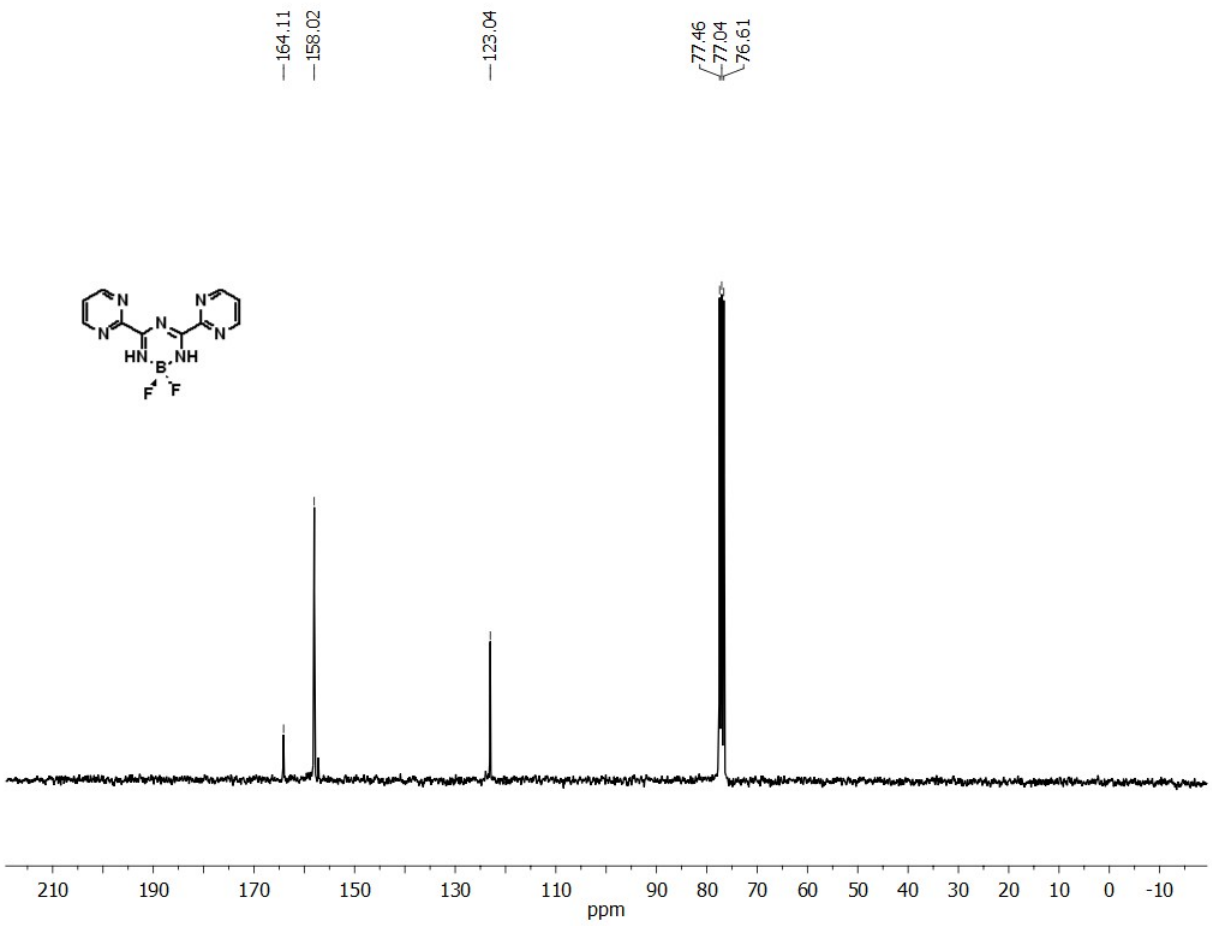

Figure S6. ^{13}C NMR spectrum of **F_2-Pm_2BTA** in $CDCl_3$

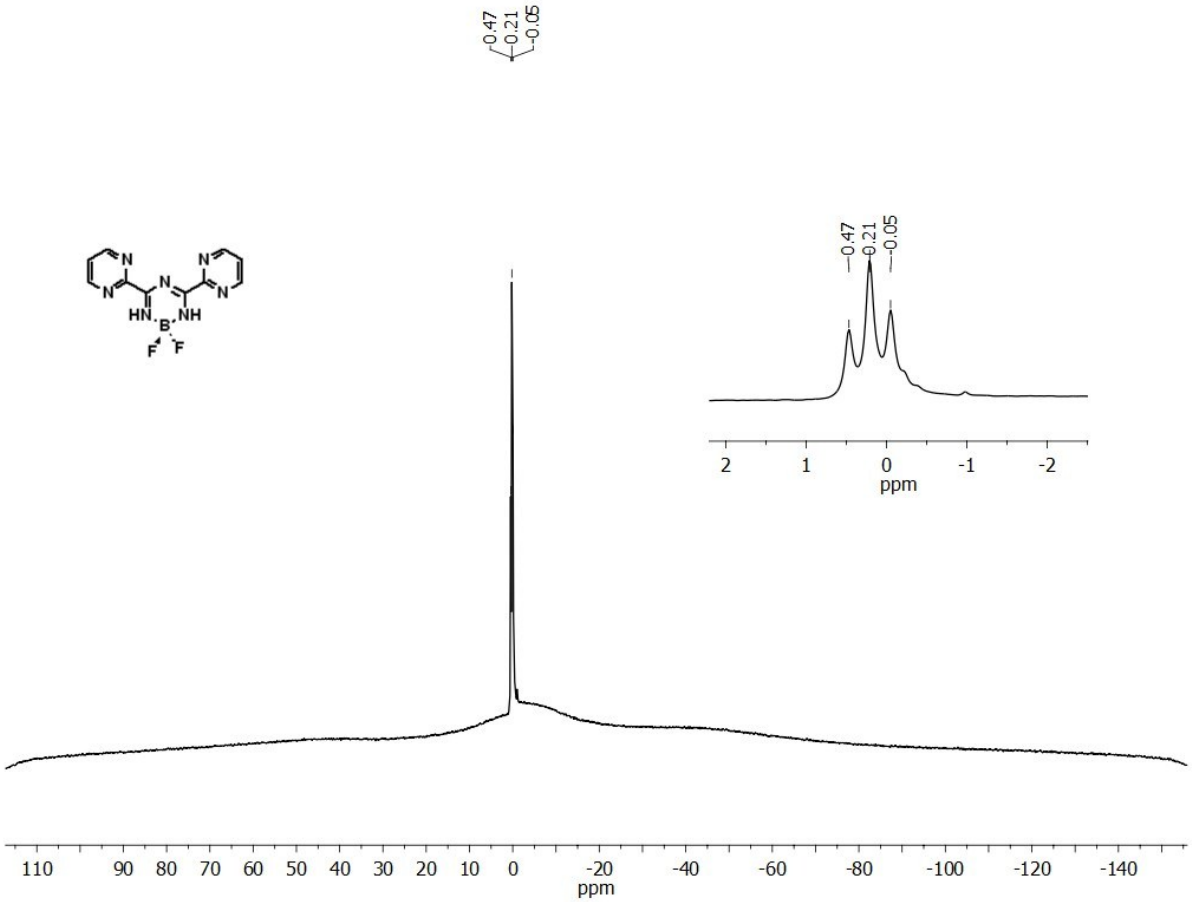

Figure S7. ^{11}B NMR spectrum of **F_2-Pm_2BTA** in $CDCl_3$

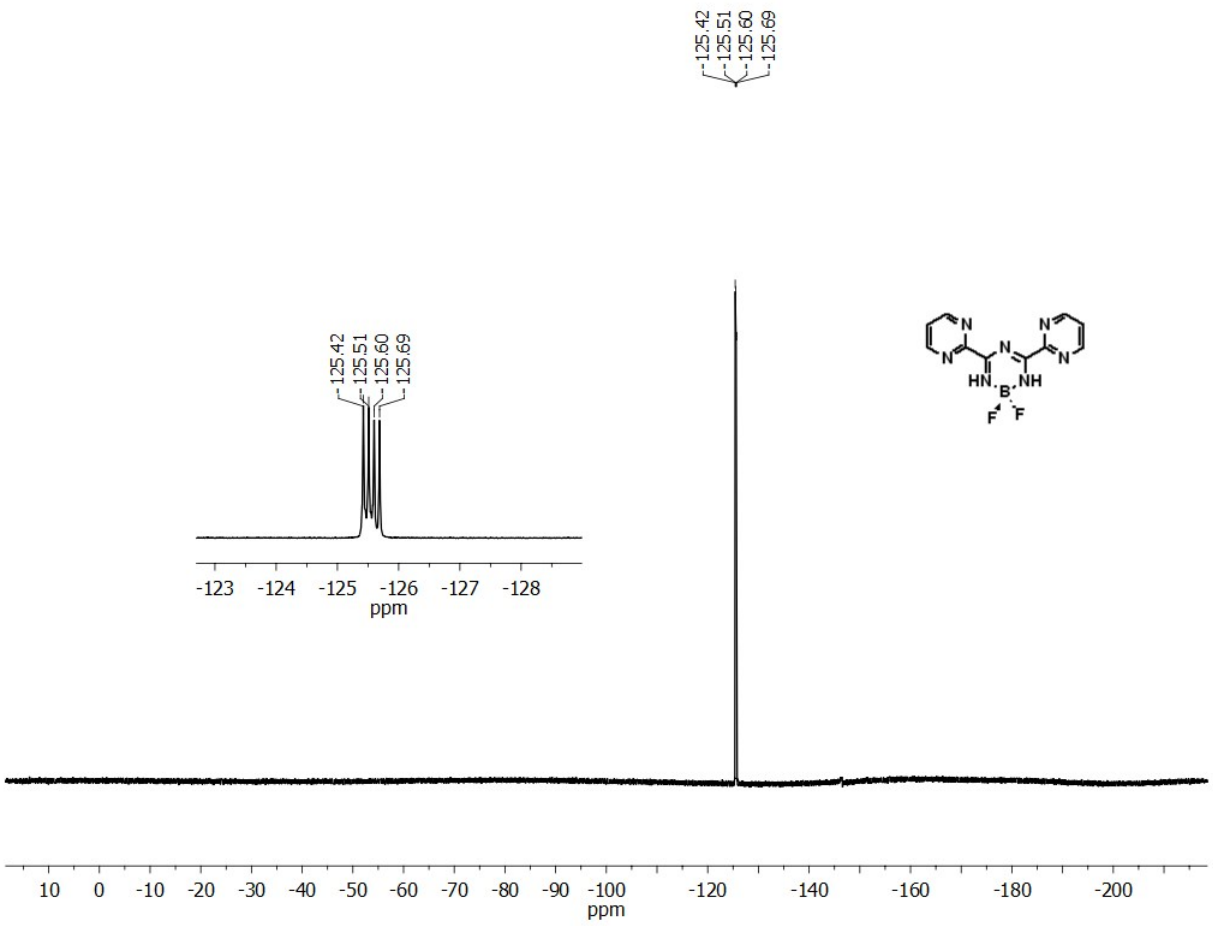

Figure S8. ^{19}F NMR spectrum of **F_2-Pm_2BTA** in $CDCl_3$

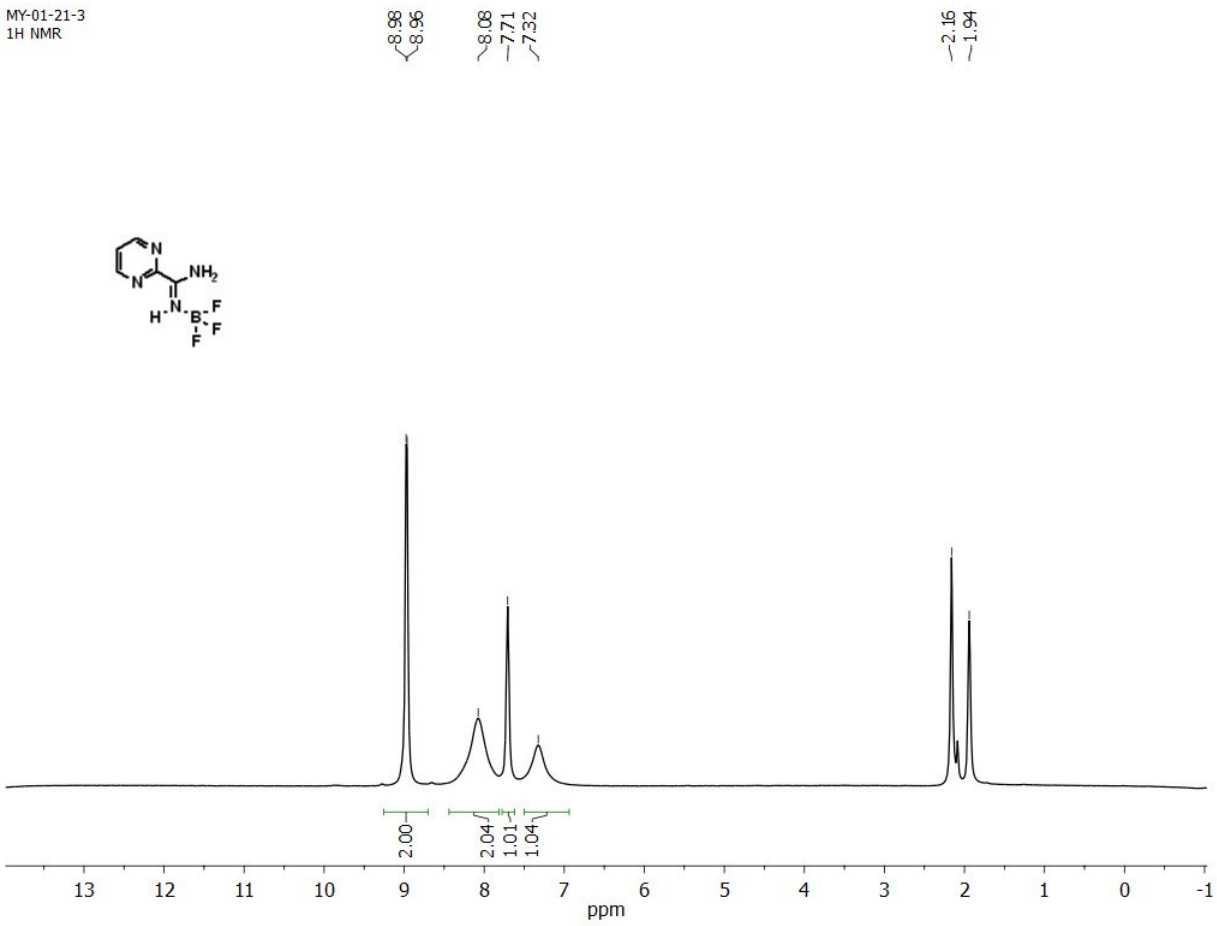

Figure S9. ^{1}H NMR spectrum of **PmAmBF$_3$** in CD_3CN

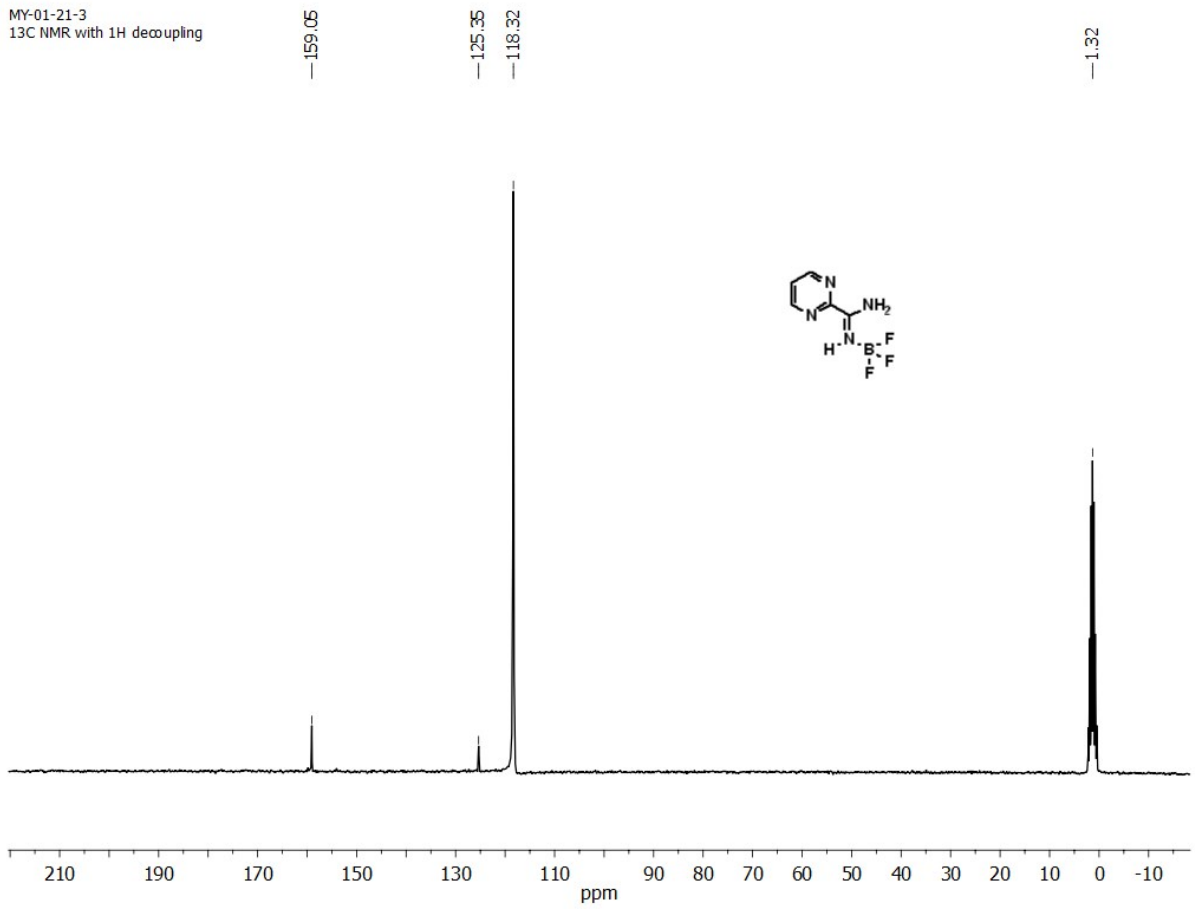

Figure S10. ^{13}C NMR spectrum of **PmAmBF$_3$** in CD_3CN

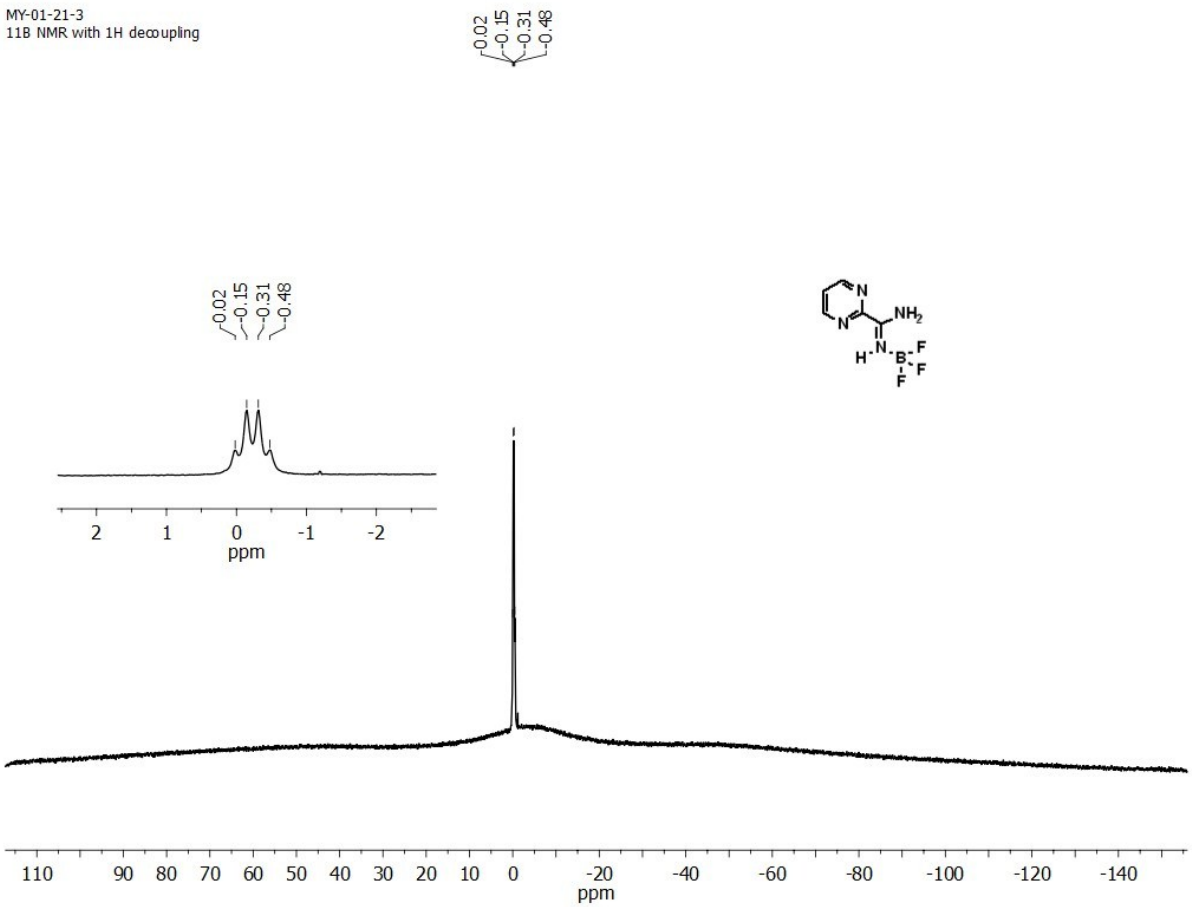

Figure S11. ^{11}B NMR spectrum of **PmAmBF$_3$** in CD_3CN

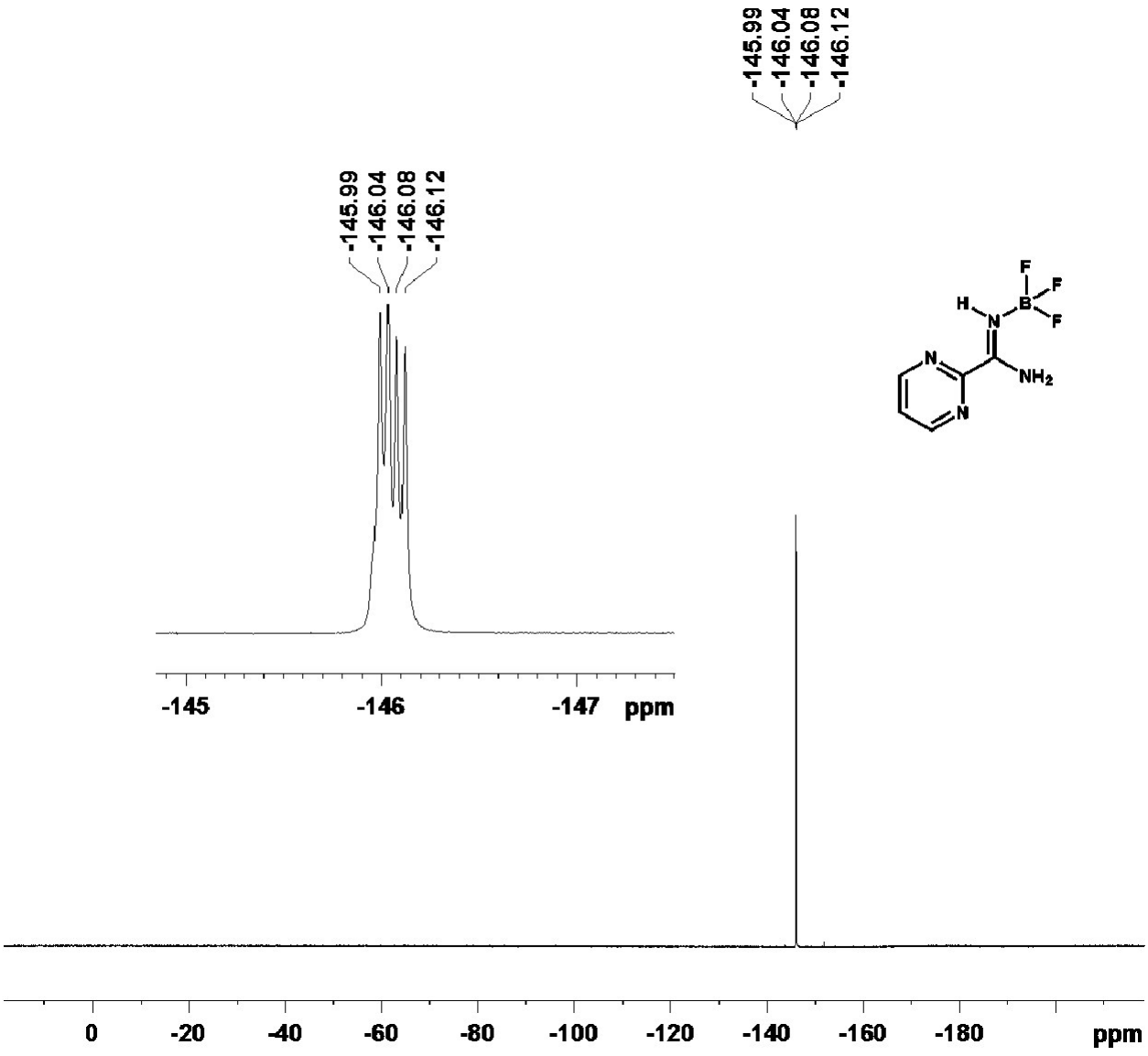

Figure S12. ^{19}F NMR spectrum of **PmAmBF$_3$** in CD_3CN

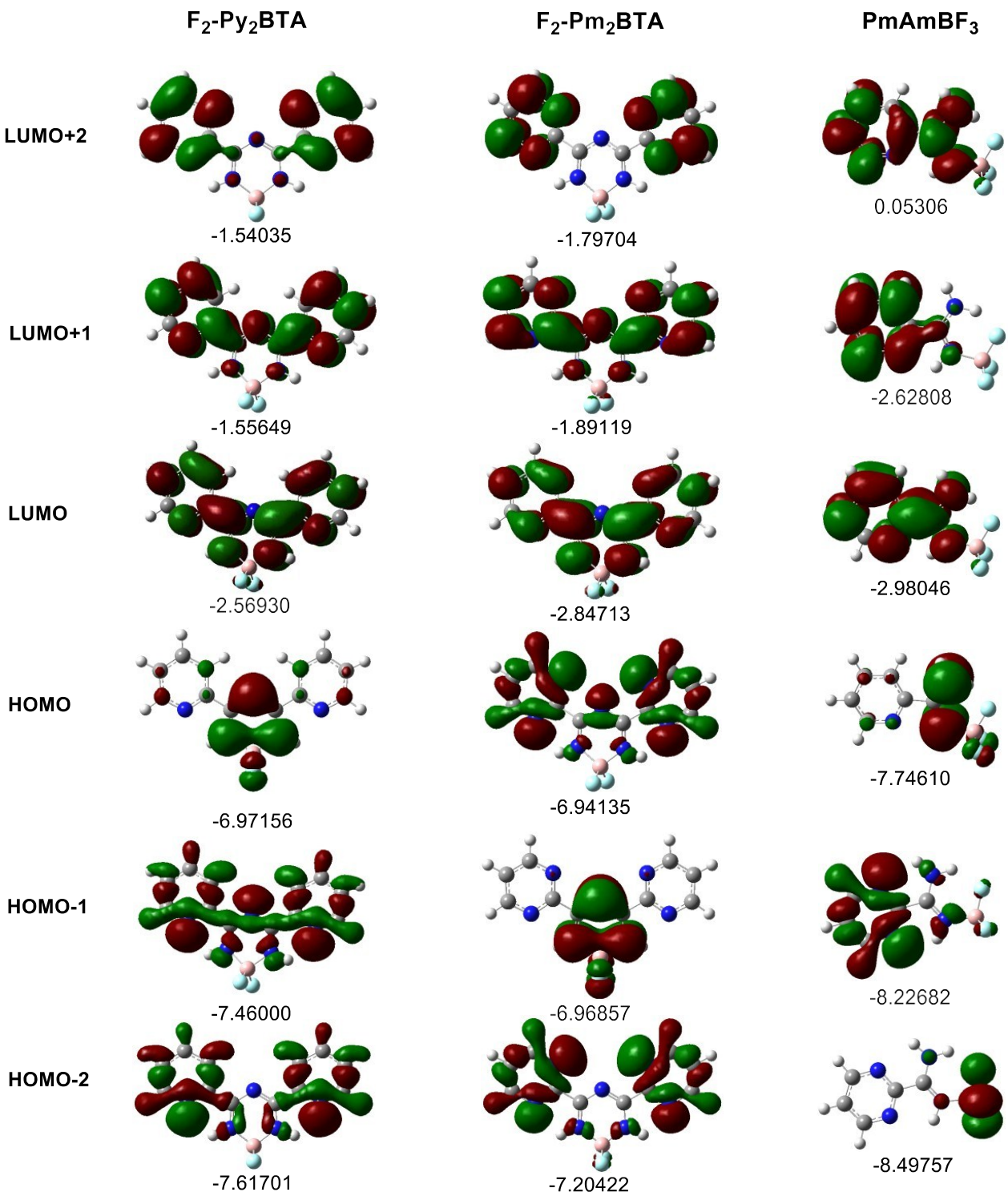

Figure S13. Frontier molecular orbitals and energies of the **F_2-Py_2BTA**, **F_2-Pm_2BTA** and **$PmAmBF_3$** from DFT calculations (B3LYP, 6-31G).

Table S1. Fluorescence data for the benchmark fluorophores **F_2-Py_2BTA** and **F_2-Pm_2BTA**.

Compound	*Absorption*[a]		*Fluorescence*[b]	
	λ_{max} *(nm)*	*($\varepsilon \times 10^4$ $LM^{-1}cm^{-1}$)*	λ_{em} *(nm)*	Quantum Yield[c]
F_2-Py_2BTA	310	2.3	397	0.12
F_2-Pm_2BTA	307	1.4	388	0.07

[a] low energy absorption of **F_2-Py_2BTA** and **F_2-Pm_2BTA** in DCM from UV-Vis. [b] Measurements were made in DCM (dichloromethane). [c] Quantum yield were calculate at 22°C relative to 9,10-diphenylanthracene in ethanol (QY = 0.90) using Cary Eclipse Fluorescence Spectrophotometer (Agilent Technologies).

Table S2. Molar extinction coefficients (ε) of **F_2-Py_2BTA**, **F_2-Pm_2BTA** and **$PmAmBF_3$** along with their corresponding wavelengths.

F_2-Py_2BTA		**F_2-Pm_2BTA**		**$PmAmBF_3$**	
λ_{abs} *(nm)*	ε *($LM^{-1}cm^{-1}$)*	λ_{abs} *(nm)*	ε *($LM^{-1}cm^{-1}$)*	λ_{abs} *(nm)*	ε *($LM^{-1}cm^{-1}$)*
324	19720	317	12720	320	489
310	22795	307	14015	304	635
280	11580	295	10776	227	7533

Table S3. TD–DFT optical transitions[a] for **F_2-Py_2BTA**, **F_2-Pm_2BTA** and **$PmAmBF_3$**.

	F_2-Py_2BTA		**F_2-Pm_2BTA**		**$PmAmBF_3$**	
k	E(eV)	*f*	E(eV)	*f*	E(eV)	*f*
1	4.1154	0.4515	3.5015	0.0000	4.1920	0.0000
2	4.1370	0.0000	3.7135	0.0000	4.5825	0.0055
3	4.3078	0.0024	4.0622	0.2796	4.8527	0.0664
4	4.6294	0.1542	4.3130	0.0000	5.0795	0.0039
5	4.6927	0.0965	4.4048	0.0089	5.6628	0.0135
6	4.7077	0.0000	4.4084	0.0000	5.7256	0.3731
7	5.1376	0.0001	4.6683	0.0010	5.8142	0.0028
8	5.1890	0.0001	4.8624	0.0606	6.2399	0.0001
9	5.2176	.0233	4.9013	0.0000	6.2595	0.0019
10	5.3439	0.0041	4.9560	0.2215	6.4273	0.0002
11	5.3793	0.0000	4.9703	0.0587	6.9605	0.0398
12	5.3843	0.0020	5.0603	0.0788	6.9847	0.0001
13	5.4987	0.0277	5.0756	0.0198	7.0065	0.0004
14	5.5133	0.0016	5.2797	0.0030	7.0711	0.2130
15	5.5333	0.0000	5.2859	0.0000	7.0988	0.0134
16	5.5612	0.2197	5.2865	0.0000	7.3725	0.0000
17	5.6601	0.0188	5.4050	0.0000	7.4656	0.4011
18	5.7248	0.0010	5.5061	0.0046	7.6039	0.0123
19	5.9429	0.0004	5.5069	0.0153	7.6157	0.0008
20	5.9517	0.0297	5.5306	0.0019	7.6971	0.0000

[a] TD-DFT (6-31G/B3LYP) level of theory on geometry optimized structures. k is order of excitation energy and *f* is oscillator strength.

Table S4. Selected TD–DFT optical transitions for **F_2-Py_2BTA**, **F_2-Pm_2BTA** and **PmAmBF_3**.

Compound	Excitation Energy (eV)	Calculated λ (nm)	Transition	Molecular Contribution	Oscillator Strength (*f*)
F_2-Py_2BTA	4.1154	301	HOMO → LUMO	0.69836	0.4515
	4.6294	267	HOMO-1 → LUMO	0.69018	0.1542
	4.6927	264	HOMO-3 → LUMO	0.68831	0.0965
F_2-Pm_2BTA	4.0622	305	HOMO-1 → LUMO	0.70295	0.2796
	4.8624	254	HOMO-3 → LUMO HOMO-1 → LUMO+1	0.55938 -0.37579	0.0606
	4.9560	250	HOMO-4 → LUMO HOMO-1 → LUMO+2	0.65539 -0.24728	0.2215
PmAmBF_3	4.5827	255	HOMO → LUMO	0.70088	0.0664
	5.7256	216	HOMO-2 → LUMO	0.68647	0.3731
	7.4656	175	HOMO-5 → LUMO HOMO-2 → LUMO+1	0.52270 0.37437	0.2130

Table S5. Crystallographic data for **F_2-Py_2BTA, F_2-Pm_2BTA** and **PmAmBF_3**.

	F_2-Py_2BTA	**F_2-Pm_2BTA**	**PmAmBF_3**
Formula	$C_{12}H_{10}BF_2N_5$	$C_{10}H_8BF_2N_7$	$C_5H_6BF_3N_4$
FW (g/mol)	273.06	359.97	189.95
Crystem System	Triclinic	Orthorhombic	Monoclinic
Space Group	*P-1*	*Pbca*	*P-2$_1$/n*
a (Å)	7.7785 (3)	9.7915(7)	8.1901(2)
b (Å)	8.8782(3)	10.7841(8)	6.2150(2)
c (Å)	9.6210(4)	28.665(2)	14.8496(4)
α (°)	91.401(2)	90	90
β (°)	102.708(2)	90	92.216(2)
γ (°)	109.795(2)	90	90
V (Å^3)	606.289(4)	3026.8(4)	755.30(4)
Z	2	8	4
D_{calc} (Mg·m^{-3})	1.496	1.580	1.670
T(K)	200	200	200
μ (mm^{-1})	0.116	0.459	0.159
2θ range (°)	4.36 to 57.99	5.038 to 51.998	5.49 to 57.99
No. of total reflections	10741	13127	6752
No. of unique reflections	3153	2913	1873
R_{int}	0.0268	0.0608	0.0163
R_1, wR_2 [I>=2σ (I)]	0.0535, 0.1579	0.0692, 0.1794	0.0341, 0.0975
Largest diff. peak/hole (e·Å-3)	0.518 and -0.186	0.289 and -0.459	0.253 and -0.184